



Contents lists available at ScienceDirect

Spectrochimica Acta Part A: Molecular and Biomolecular Spectroscopy

journal homepage: www.elsevier.com/locate/saa

Synthesis and characterization of 2,2'-(pyridine-2,6-diyl)bis(1*H*-benzo[*d*]imidazol-3-ium) 2,4,6-trimethylbenzenesulfonate chloride by experimental and theoretical methods



Namık Özdemir^{a,*}, Osman Dayan^{b,*}, Melek Tercan Yavaşoğlu^b, Bekir Çetinkaya^c

^a Department of Physics, Faculty of Arts and Sciences, Ondokuz Mayıs University, 55139 Samsun, Turkey

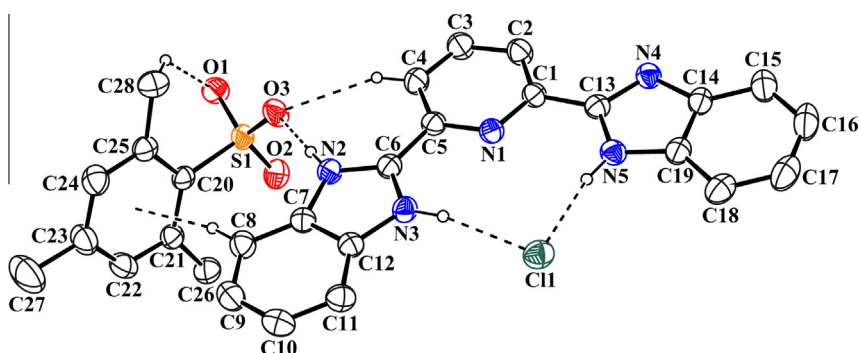
^b Laboratory of Inorganic Synthesis and Molecular Catalysis, Çanakkale Onsekiz Mart University, 17020 Çanakkale, Turkey

^c Department of Chemistry, Faculty of Science, Ege University, 35100 İzmir, Turkey

HIGHLIGHTS

- A novel benzimidazole compound was synthesized unexpectedly.
- The compound was crystallized as salt.
- The structure of the compound was determined by X-ray crystallography.
- The compound was characterized by FT-IR, NMR and UV–vis. spectroscopy.
- The structure and spectroscopic properties were examined by DFT method.

GRAPHICAL ABSTRACT



ARTICLE INFO

Article history:

Received 11 November 2013
 Received in revised form 2 March 2014
 Accepted 23 April 2014
 Available online 5 May 2014

Keywords:

Crystal structure
 FT-IR
 NMR
 UV–vis.
 DFT calculations

ABSTRACT

The title molecular salt (**2**), 2,2'-(pyridine-2,6-diyl)bis(1*H*-benzo[*d*]imidazol-3-ium) 2,4,6-trimethylbenzenesulfonate chloride ($C_{19}H_{15}N_5^{2+} \cdot C_9H_{11}O_3S^- \cdot Cl^-$), was synthesized unexpectedly from the reaction of 2,6-bis(benzimidazol-2-yl)pyridine (**1**) with 2-mesitylenesulfonyl chloride. Spectroscopic techniques (FT-IR, NMR and UV–vis.) were used to characterize compounds **1** and **2**. Solid-state structure of compound **2** was identified by X-ray crystallography. Theoretical characterization of the spectroscopic properties of compounds **1** and **2** was achieved using the density functional theory (DFT) method with the 6-311G(d,p) basis set, and the results were checked against the experimental data. Electronic absorption spectra of the compounds have also been obtained.

© 2014 Elsevier B.V. All rights reserved.

Introduction

N-heterocyclic ligands have recently become more attractive in applied chemistry [1–3]. The most common of these is a group of

benzimidazole, which is very attractive with its weak π -receptor and strong π -donor property. One of the unpaired electron pairs contributes the aromatic ring and the other one gives molecule basic character [4]. So that, nitrogen atom enables substitution and changing electronic and steric properties of the molecule [5]. Benzimidazole derivatives have been investigated intensively in view of application of biological activity such as inhibition of topoisomerase I, antifungal, antiparasitic, anticancer and antimicrobial effect [6–14].

* Corresponding authors. Tel.: +90 362 3121919/5256; fax: +90 362 4576081 (N. Özdemir). Tel.: +90 286 2180018/1860; fax: +90 28621805333 (O. Dayan).

E-mail addresses: namiko@omu.edu.tr (N. Özdemir), osmandayan@comu.edu.tr (O. Dayan).

On the other hand, tridentate N-compounds bearing benzimidazolyl/pyridine rings are very stable because of their π electrons. The usability of these compounds and their derivatives in the field of optical sensors, solar energy conversion systems, electronic devices, etc. depends on the control of the features of compounds geometry, photo-physical/-chemical and electrochemical properties [15,16]. Particularly, 2,6-bis(benzimidazol-2-yl)pyridine (bizimpy) and its metal complexes are used in many applications such as biochemistry [17], electrochemistry [18,19] and catalysis [20–23]. 2,6-Bis(benzimidazol-2-yl)pyridines like other benzimidazoles are easily substituted with the reaction of alkyl halides in basic conditions. However, in this work, we show that a new pyridinium salt has been synthesized with the reaction of 2,6-bis(benzimidazol-2-yl)pyridine and 2-mesitylenesulfonyl chloride in basic conditions.

We report here results of a detailed study of the synthesis and characterization of bizimpy and title compound using IR, NMR (^1H and ^{13}C NMR) and UV–vis. spectroscopies and quantum chemical methods. The density functional theory at the B3LYP/6-311G(d,p) level was employed for the theoretical characterization of the both compounds. The crystal structure of the title compound was also determined by single-crystal X-ray diffraction experiment.

Materials and methods

General remarks

All reagents and solvents were obtained from commercial suppliers and used without further purification. Melting points were determined in open capillary tubes on a digital Stuart SMP10 melting point apparatus. NMR spectra were recorded at 297 K on a Varian Mercury AS 400 NMR spectrometer at 400 MHz (^1H), 100.56 MHz (^{13}C) in $\text{DMSO}-d_6$ with TMS as the internal standard. Infrared spectra were measured with a Perkin Elmer SpectrumOne FTIR system and recorded using a universal ATR sampling accessory within the range 4000–650 cm^{-1} . UV–vis. spectra were recorded with a Perkin Elmer Lambda 25 UV–vis. spectrometer.

Syntheses

Bizimpy (1)

Bizimpy was synthesized according to published procedures [24]. Pyridine-2,6-dicarboxylic acid (dipicolinic acid) (20 mmol, 3.35 g) was added to 1,2-phenylenediamine (44 mmol, 4.7 g) in phosphoric acid (40 ml). The reaction mixture was stirred during 4 h under Ar atmosphere. The obtained green–blue melt was poured into ice and after reaching room temperature, filtered off. Then sodium carbonate (10%, 100 ml) solution was added to the filtrate. After recrystallization from methanol, white-beige crystals were obtained. Yield: 68% melting point: 626 K.

2,2'-(Pyridine-2,6-diyl)bis(1H-benzo[d]imidazol-3-ium) 2,4,6-trimethylbenzenesulfonate chloride (2)

Bizimpy (3.21 mmol, 1 g) was dissolved in THF (20 ml). Potassium hydroxide (6.42 mmol, 0.36 g) was added to this solution and refluxed for 2 h. 2-Mesitylenesulfonyl chloride (6.42 mmol, 1.40 g, in THF) was added to the reaction mixture and refluxed for 12 h (Fig. 1). After removing solvent, the obtained solid was washed with brine and extracted with CH_2Cl_2 (20 ml \times 3). X-ray quality crystals were grown from dichloromethane/hexane (1:3). Yield: 70% melting point: 562 K (dec.).

X-ray crystallography

The intensity data of the title compound were collected on a STOE diffractometer with an IPDS II image plate detector at room

temperature (296 K) using graphite monochromated Mo $K\alpha$ radiation ($\lambda = 0.71073 \text{ \AA}$) in ω -scanning mode. The structure was solved by direct methods using SHELXS-97 [25] and refined through the full-matrix least-squares method using SHELXL-97 [26] implemented in the WinGX [27] program suite. Carbon bound hydrogen atoms were positioned geometrically and treated using a riding model, fixing the bond lengths at 0.93 and 0.96 \AA for CH and CH_3 atoms, respectively, while the nitrogen bound hydrogen atoms were located in a difference Fourier map and refined isotropically [$\text{N}-\text{H} = 0.85(2)-0.90(2) \text{ \AA}$]. Data collection: X-AREA [28], cell refinement: X-AREA, data reduction: X-RED32 [28]. Details of the data collection conditions and the parameters of refinement process are given in Table 1. The general-purpose crystallographic tool PLATON [29] was used for the structure analysis and presentation of the results. The molecular graphics were done using ORTEP-3 for Windows [30].

Computational technique

All geometries were fully optimized in the ground state using the Berny algorithm [31,32] without symmetry restrictions and using the default convergence criteria. The calculations were performed by means of the Gauss-View molecular visualization program [33] and Gaussian 03W program package [34] using the density functional theory (DFT) [35] with the three-parameter hybrid functional (B3) [36] for the exchange part and the Lee–Yang–Parr (LYP) correlation function [37], denoted B3LYP, at 6-311G(d,p) [38,39] basis set. All the geometry optimizations were followed by frequency calculations and no imaginary frequencies were found, approving the stable nature of the optimized structures. A scale factor of 0.9679 [40] was used to correct the calculated vibrational frequencies. The ^1H and ^{13}C NMR chemical shifts were calculated within the gauge-independent atomic orbital (GIAO) approach [41,42] applying the same method and the basis set as used for geometry optimization. The ^1H and ^{13}C NMR chemical shifts were converted to the TMS scale by subtracting the calculated absolute chemical shielding of TMS ($\delta = \Sigma_0 - \Sigma$, where δ is the chemical shift, Σ is the absolute shielding and Σ_0 is the absolute shielding of TMS), whose value are 31.99 and 185.06 ppm, respectively. The effect of solvent on the theoretical NMR parameters was included using the default model IEF-PCM (Integral-Equation-Formalism Polarizable Continuum Model) [43] provided by Gaussian 03W. DMSO was used as solvent. The electronic absorption spectra were calculated using the time-dependent density functional theory (TD-DFT) method [44,45].

Results and discussion

Description of crystal structure

The title compound (2), an ORTEP-3 view of which is shown in Fig. 2, crystallizes as a salt in the monoclinic system $P2_1/c$ with $Z = 4$, and composed of a 2,2'-(pyridine-2,6-diyl)bis(1H-benzo[d]imidazol-3-ium) cation, a 2,4,6-trimethylbenzenesulfonate anion and one chloride anion.

The 2,2'-(pyridine-2,6-diyl)bis(1H-benzo[d]imidazol-3-ium) cation is essentially planar with the largest individual deviation from planarity of 0.0938(17) \AA for atom N3, while the benzene ring plane of the 2,4,6-trimethylbenzenesulfonate anion is almost perpendicular to this plane with an angle of 78.349(64) $^\circ$. In the 2,4,6-trimethylbenzenesulfonate anion, the methyl group showing the greatest deviation from the least-squares plane of the aromatic ring in the anion is that *para* to the sulfonate group, with a value of 0.0348(32) \AA , while atom S1 deviates from the plane of the aromatic ring by 0.0250(18) \AA . The aromatic C–C and C–N distances and bond angles in both the benzimidazole and pyridine rings

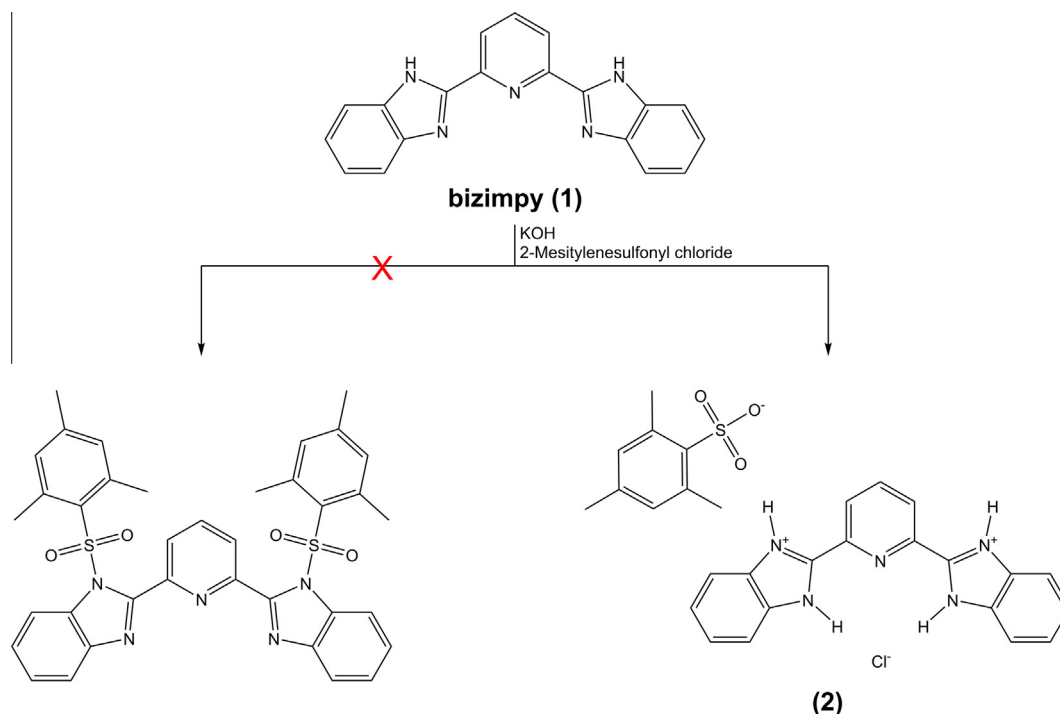


Fig. 1. Formation of the title compound.

Table 1
Crystal data and structure refinement parameters for the title compound.

CCDC deposition no.	802607
Color/shape	Colorless/prism
Chemical formula	$C_{19}H_{15}N_5^{2+} \cdot C_9H_{11}O_3S^- \cdot Cl^-$
Formula weight	548.05
Temperature (K)	296
Wavelength (Å)	0.71073 Mo K α
Crystal system	Monoclinic
Space group	$P2_1/c$ (No. 14)
Unit cell parameters	
<i>a</i> , <i>b</i> , <i>c</i> (Å)	18.5426(12), 8.2193(4), 20.5076(12)
α , β , γ (°)	90, 118.047(5), 90
Volume (Å ³)	2758.5(3)
<i>Z</i>	4
<i>D</i> _{calc} (g/cm ³)	1.320
μ (mm ⁻¹)	0.253
Absorption correction	Integration
<i>T</i> _{min} , <i>T</i> _{max}	0.9704, 0.8849
<i>F</i> ₀₀₀	1144
Crystal size (mm ³)	0.80 × 0.39 × 0.14
Diffractometer/measurement method	STOE IPDS II/ ω scan
Index ranges	$-23 \leq h \leq 23$, $-10 \leq k \leq 10$, $-24 \leq l \leq 25$
θ range for data collection (°)	$1.99 \leq \theta \leq 26.61$
Reflections collected	14635
Independent/observed reflections	5698/3242
<i>R</i> _{int}	0.0484
Refinement method	Full-matrix least-squares on <i>F</i> ²
Data/restraints/parameters	5698/0/366
Goodness-of-fit on <i>F</i> ²	1.004
Final <i>R</i> indices [<i>I</i> > 2 σ (<i>I</i>)]	<i>R</i> ₁ = 0.0440, <i>wR</i> ₂ = 0.0713
<i>R</i> indices (all data)	<i>R</i> ₁ = 0.0951, <i>wR</i> ₂ = 0.0786
$\Delta\rho_{max}$, $\Delta\rho_{min}$ (e/Å ³)	0.164, -0.229

are within the usual ranges [46–49], confirming the aromatic character of the pyridine and benzimidazole moieties. The positions of N2 and N4 atoms are *trans*–*trans* with respect to pyridine N1 atom, and the protonation of these atoms has no effect on the aromatic character of the two benzimidazole moieties. The geometry of

the 2,4,6-trimethylbenzenesulfonate anion shows also good agreement with those previously reported [50,51].

In the molecular structure of the 2,4,6-trimethylbenzenesulfonate anion, there is a C28–H28A···O1 intramolecular interaction leading to the formation of a six-membered ring with graph-set descriptor *S*(6) [52]. In the crystal structure, there are extensive cation···anion intermolecular interactions. Each 2,2'-(pyridine-2,6-diyl)bis(1*H*-benzo[*d*]imidazol-3-ium) cation is hydrogen bonded to both the chloride anion *via* a pair of N–H···Cl hydrogen bonds in an *R*₂¹(10) motif, and the 2,4,6-trimethylbenzenesulfonate anion *via* the N2–H2···O3 and C4–H4A···O3 hydrogen bonds in an *R*₂¹(7) motif [52]. There is also a C–H··· π (arene) interaction between the 2,2'-(pyridine-2,6-diyl)bis(1*H*-benzo[*d*]imidazol-3-ium) cation and 2,4,6-trimethylbenzenesulfonate anion. In addition, atoms N4 and C2 in the molecule at (*x*, *y*, *z*) act as hydrogen-bond donors, respectively, to atoms O1 and O3 in the molecule at ($-x$, *y* – 1/2, $-z$ + 3/2), so forming an *R*₂²(9) ring (see Fig. S1 in Supplementary materials). Finally, atom C17 in the molecule at (*x*, *y*, *z*) acts as hydrogen-bond donor to atom O2 in the molecule at ($-x$, $-y$, $-z$ + 1). The full geometry of these interactions is given in Table 2.

Theoretical structure

The optimized parameters (bond lengths, bond angles, and dihedral angles) of the title compound have been obtained using the B3LYP/6-311G(d,p) method. Some selected geometrical parameters experimentally obtained and theoretically calculated are listed in Table 3.

From Table 3, one can easily say that agreement between the calculated and experimental structures is sufficient. The largest deviations in the bond distances are observed in S–O₃ bonds of the 2,4,6-trimethylbenzenesulfonate anion probably due to hydrogen bonding interactions. Similarly, the largest deviation of bond angles appears to be 1.69° at O1–S1–C20. Although the 2,2'-(pyridine-2,6-diyl)bis(1*H*-benzo[*d*]imidazol-3-ium) cation is planar in its solid state, this is not observed in the obtained theoretical structure. The benzimidazole ring planes are tilted with respect to

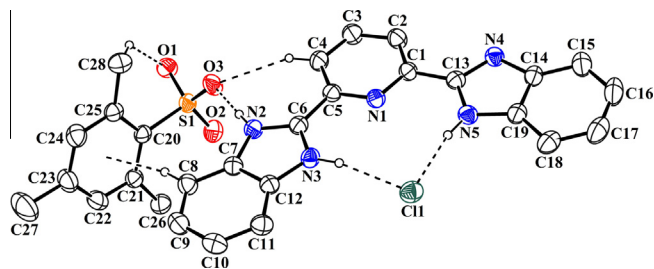


Fig. 2. A view of the title compound showing the atom-numbering scheme. Displacement ellipsoids are drawn at the 30% probability level and H atoms are shown as small spheres of arbitrary radii. Hydrogen bonds are shown as dashed lines. For the sake of clarity, only hydrogen atoms involved in hydrogen bonding have been included.

Table 2
Hydrogen bonding geometry for the title compound.

D—H...A	D—H (Å)	H...A (Å)	D...A (Å)	D—H...A (°)
C28—H28A...O1	0.96	2.46	3.162(3)	129
N2—H2...O3	0.90(2)	1.80(2)	2.699(2)	179(2)
N3—H3...C11	0.88(2)	2.30(2)	3.164(2)	168.8(18)
N5—H5...C11	0.88(2)	2.22(2)	3.0816(19)	166(2)
C8—H8...Cg	0.93	2.72	3.625(3)	165
C2—H2A...O3 ^a	0.93	2.44	3.337(3)	161
C4—H4A...O3	0.93	2.45	3.314(3)	155
N4—H4...O1 ^a	0.85(2)	1.88(2)	2.668(2)	153(2)
C17—H17...O2 ^b	0.93	2.51	3.358(3)	152

Cg: the centroid of the C20–C25 ring.

^a $-x, y - 1/2, -z + 3/2$,

^b $-x, -y, -z + 1$.

the central pyridine ring by angles of 13.04° and 9.76° for N2/N3/C6–C12 and N4/N5/C13–C19, respectively, while the dihedral angle between the 2,2'-(pyridine-2,6-diyl)bis(1*H*-benzo[*d*]imidazol-3-ium) cation and 2,4,6-trimethylbenzenesulfonate anion is 72.16°.

To globally compare the experimental and theoretical structures, these structures are overlapped with each other, giving RMSE's of 0.155 and 0.603 Å for the 2,2'-(pyridine-2,6-diyl)bis(1*H*-benzo[*d*]imidazol-3-ium) cation and 2,4,6-trimethylbenzenesulfonate anion, respectively (see Fig. S2 in Supplementary materials). The large RMSE value obtained for the anion can be explained by the intermolecular interactions in the crystal structure.

Vibrational spectra

The experimental FT-IR spectra of compounds **1** and **2** are shown in Fig. 3. Harmonic vibrational frequencies of the compounds were computed at the B3LYP/6-311G(d,p) level and the vibrational band assignments were done by means of the Gauss-View molecular visualization program. Comparison of the observed and calculated vibrational frequencies is given in Table 4. From the table, it is seen that there exists an acceptable agreement between the experimental and theoretical vibrational frequencies.

It is reported that the N–H stretching band is usually observed in the region 3300–3500 cm⁻¹ [53]. In the IR spectra of compound **1**, the peak at 3181 cm⁻¹ represents to secondary amine N–H stretching vibration that has been calculated at 3539 cm⁻¹. The corresponding stretching frequency for compound **2** is seen as two bands at 3242 and 2733 cm⁻¹ while these were calculated at 3535 and 2905 cm⁻¹, respectively. The N–H in-plane bending vibration is assigned to the wavenumber at 1385 and 1230 cm⁻¹ for compound **1** and at 1352 cm⁻¹ for compound **2**, that have been calculated at 1378, 1193 and 1363 cm⁻¹, respectively. We could

not observe the N–H out-of-plane bending vibration in the FT-IR spectra of compound **1**. However, this band is observed at 960 and 881 cm⁻¹ for compound **2** and appeared at 993 and 883 cm⁻¹, respectively, in the theoretical spectra.

It is stated the C–H stretching, C–H in-plane bending and C–H out-of-plane bending vibrations of the aromatic compounds appear in 2900–3150, 1100–1500 and 750–1000 cm⁻¹ frequency ranges, respectively [54]. The C–H aromatic stretching modes were recorded at 3111 and 3064 cm⁻¹ for compound **1** and at 3058 and 3034 cm⁻¹ for compound **2** experimentally and were computed at 3095 and 3073 cm⁻¹ for compound **1** and at 3052 and 3048 cm⁻¹ for compound **2**, respectively. The C–H in-plane bending vibrations predicted at 1427, 1413 and 1132 cm⁻¹ for compound **1** and at 1415 cm⁻¹ for compound **2** by B3LYP/6-311G(d,p) method show good agreement with FT-IR bands at 1457, 1434 and 1150 cm⁻¹ for compound **1** and at 1411 cm⁻¹ for compound **2**. The C–H out-of-plane bending vibrations are identified at 925, 815 and 738 cm⁻¹ for compound **1** and at 850, 739 and 719 cm⁻¹ for compound **2**, and these frequencies are found to be well within their characteristic regions.

The C–H stretching vibrations of methyl groups occurs at lower frequencies than those of aromatic ring. Moreover, the asymmetric mode is usually at higher wavenumber than the symmetric mode. In this work, the C–H₃ symmetric stretching frequencies of compound **2** are assigned at 2929 and 2853 cm⁻¹, whereas the C–H₃ asymmetric frequency is assigned at 2969 cm⁻¹. These bands are calculated as 2947, 2924 and 2973 cm⁻¹. The peak at 1454 cm⁻¹ is assigned to the C–H₃ scissoring vibration whereas the peaks at 1031 and 1001 cm⁻¹ are assigned to the C–H₃ wagging and twisting vibrations, respectively, in FT-IR.

Azomethine (C=N) bond stretching vibration was observed at 1490 cm⁻¹ for compound **1** and at 1621 cm⁻¹ for compound **2** experimentally, while these were calculated at 1521 and 1615 cm⁻¹, respectively. The band at 1576 cm⁻¹ in the FT-IR spectra of compound **1** and the bands at 1564 and 1522 cm⁻¹ in the FT-IR spectra of compound **2**, which can be attributed to the ring C=C stretching vibrations, were calculated at 1571, 1580 and 1555 cm⁻¹ for B3LYP, respectively.

Asymmetric vibrations of SO₃⁻ group of sulfonic acid salts usually occur in the FT-IR at 1250–1140 cm⁻¹. The band due to the symmetric stretching vibration is sharper and occurs at 1130–1080 cm⁻¹ [53]. We calculated the asymmetric and symmetric S–O₃ stretching vibrations at 1181 and 1061 cm⁻¹ for compound **2**, while these bands were obtained at 1153 and 1119 cm⁻¹ in the FT-IR spectra, respectively. In addition, the band at 653 cm⁻¹ in the FT-IR spectra of compound **2**, which is assigned to the C–S stretching vibration, was calculated at 641 cm⁻¹. The other experimental and theoretical vibrational frequencies can be seen in Table 4.

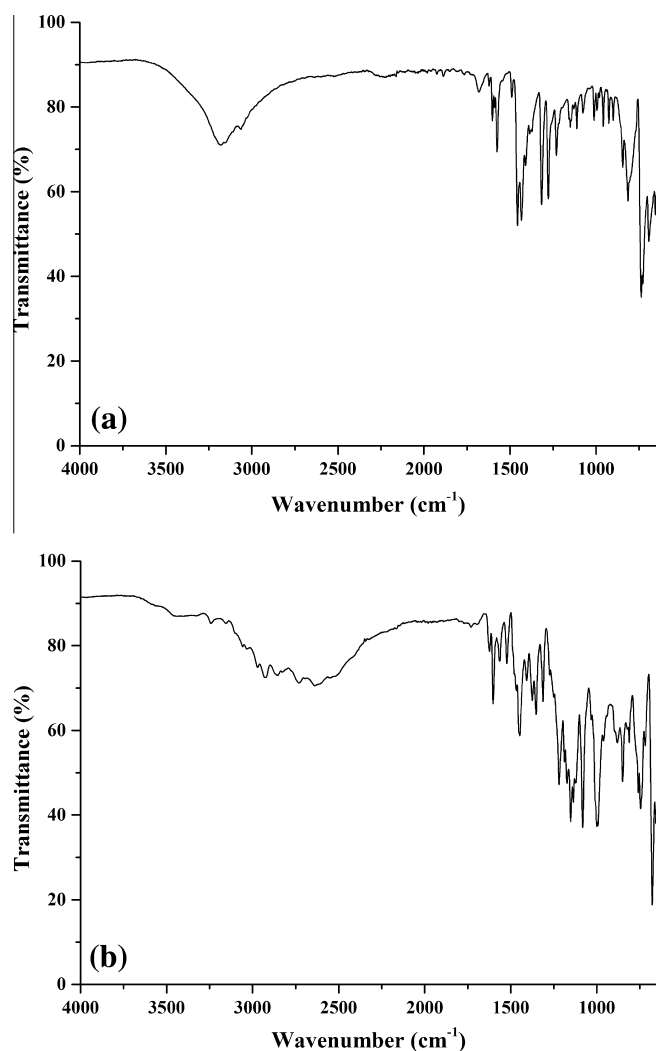
NMR spectra

The characterization of the compounds was further enhanced by the use of NMR spectroscopy. The NMR spectra of the compounds were recorded on a Varian Mercury AS 400 NMR spectrometer and shown in Figs. S3 and S4 in Supplementary materials. Theoretical ¹H and ¹³C NMR chemical shift values of the compounds have been computed using the same method and the basis set for the optimized geometry. The results of these calculations are collected in Table 5 together with the experimental values. Since experimental ¹H chemical shift values were not available for the individual hydrogen atoms of the methyl groups in compound **2**, the average of the computed values is given for these hydrogen atoms.

All NMR data are consistent with the structural formula of the compounds. In the ¹H NMR spectra of compound **1**, the chemical

Table 3
Optimized and experimental geometries of the title compound.

Parameters	Experimental	Calculated	Parameters	Experimental	Calculated
<i>Bond lengths (Å)</i>					
S1–O1	1.4543(15)	1.485	N2–C7	1.390(3)	1.383
S1–O2	1.4318(17)	1.469	N3–C6	1.333(3)	1.346
S1–O3	1.4638(17)	1.523	N3–C12	1.388(3)	1.380
S1–C20	1.780(2)	1.823	N4–C13	1.332(3)	1.356
N1–C1	1.338(2)	1.331	N4–C14	1.373(3)	1.392
N1–C5	1.324(3)	1.333	N5–C13	1.337(3)	1.329
N2–C6	1.332(3)	1.338	N5–C19	1.377(3)	1.384
<i>Bond angles (°)</i>					
O1–S1–O2	113.15(11)	114.80	C6–N2–C7	108.68(18)	108.01
O1–S1–O3	110.13(10)	109.17	C6–N3–C12	108.48(19)	108.50
O2–S1–O3	112.77(11)	112.37	C13–N4–C14	109.46(18)	109.18
O1–S1–C20	105.57(10)	107.26	C13–N5–C19	109.21(19)	109.19
O2–S1–C20	109.58(10)	108.81	N2–C6–C5	126.8(2)	127.17
O3–S1–C20	105.08(10)	103.78	N3–C6–C5	123.5(2)	122.68
N2–C6–N3	109.61(19)	110.16	N4–C13–C1	128.12(19)	126.77
N4–C13–N5	108.5(2)	108.96	N5–C13–C1	123.4(2)	124.26
C1–N1–C5	117.70(18)	118.88			
<i>Torsion angles (°)</i>					
N1–C5–C6–N2	–175.9(2)	167.58	C4–C5–C6–N2	3.3(3)	–13.50
N1–C5–C6–N3	1.6(3)	–12.59	C4–C5–C6–N3	–179.3(2)	166.33
N1–C1–C13–N4	–174.3(2)	–171.16	C2–C1–C13–N4	5.5(4)	9.84
N1–C1–C13–N5	3.8(3)	9.20	C2–C1–C13–N5	–176.5(2)	–169.80

**Fig. 3.** FT-IR spectra of compounds **1** (a) and **2** (b).**Table 4**
Comparison of the observed and calculated vibrational frequencies (cm^{-1}) for compounds **1** and **2**.

Assignments	1		2	
	Experimental	Calculated	Experimental	Calculated
ν N–H	3181	3539	3242	3535
ν_s C–H	3111	3095	3058	3052
ν_{as} C–H	3064	3073	3034	3048
ν_{as} C–H ₃	–	–	2969	2973
ν_s C–H ₃	–	–	2929	2947
ν_s C–H ₃	–	–	2853	2924
ν N–H	–	–	2733	2905
ν C=N	–	–	1621	1615
ν C=C	1576	1571	1564	1580
ν C=C	–	–	1522	1555
ν C=N	1490	1521	–	–
α C–H ₃	–	–	1454	1452
γ C–H	1457	1427	–	–
γ C–H	1434	1413	1411	1415
γ N–H	1385	1378	1352	1363
ν C–N	1317	1334	1275	1275
ν C–N	1277	1255	1219	1216
γ N–H	1230	1193	–	–
ν_{as} S–O ₃	–	–	1153	1181
ν_s S–O ₃	–	–	1119	1061
γ C–H	1150	1132	–	–
ω C–H ₃	–	–	1031	1037
δ C–H ₃	–	–	1001	1019
ω N–H	–	–	960	993
ω N–H	–	–	881	883
δ C–H	925	915	850	849
θ	844	824	811	830
θ	–	–	759	793
ω C–H	815	809	739	744
ω C–H	738	732	719	736
ν C–S	–	–	653	641

Vibrational modes: ν , stretching; α , scissoring; γ , rocking; ω , wagging; δ , twisting; θ , ring breathing. Abbreviations: as, asymmetric; s, symmetric.

shifts of $-H_{benzimidazole}$ peaks were appeared as two multiplets around 7.23–7.41 and 7.66–7.86 ppm, which have been calculated at 7.62–7.69 and 7.90–8.09 ppm, respectively. Pyridine backbone hydrogen's were observed as triplet at 8.17 ppm for $-H_{3A}$ and as doublets at 8.34 ppm for $-H_{2A,4A}$. These signals have been obtained

Table 5
Experimental and theoretical ^{13}C and ^1H NMR chemical shifts δ (ppm) from TMS for compounds **1** and **2**.

Atom	1		2	
	Experimental	Calculated	Experimental	Calculated
C1	–	–	141.86	147.16
C2	–	–	123.30	131.20
C3	–	–	145.34	148.83
C4	–	–	123.30	138.92
C5	–	–	141.86	150.86
C6	–	–	148.64	153.31
C7	–	–	115.29	141.50
C8	–	–	130.13	121.48
C9	–	–	130.13	133.12
C10	–	–	130.13	133.72
C11	–	–	130.13	120.20
C12	–	–	115.29	139.33
C13	–	–	148.64	152.66
C14	–	–	115.29	138.61
C15	–	–	130.13	119.71
C16	–	–	130.13	135.31
C17	–	–	130.13	134.17
C18	–	–	130.13	121.88
C19	–	–	115.29	139.67
C20	–	–	136.05	151.01
C21	–	–	137.02	144.00
C22	–	–	124.65	136.50
C23	–	–	139.92	148.58
C24	–	–	124.65	136.71
C25	–	–	137.02	146.68
C26	–	–	22.71	27.10
C27	–	–	20.27	23.68
C28	–	–	22.71	24.69
H2 (N2)	13.01 (br, 2H)	9.01	10.28 (br, 4H)	19.34
H3 (N3)	–	–	10.28 (br, 4H)	15.57
H4 (N4)	13.01 (br, 2H)	9.01	10.28 (br, 4H)	9.64
H5 (N5)	–	–	10.28 (br, 4H)	18.89
H2A	8.34 (d, 2H, $J = 9$ Hz)	8.03	8.52 (d, 2H, $J = 9$ Hz)	8.44
H3A	8.17 (t, 1H, $J = 9$ Hz)	8.37	8.39 (t, 1H, $J = 8.5$ Hz)	8.69
H4A	8.34 (d, 2H, $J = 9$ Hz)	8.03	8.52 (d, 2H, $J = 9$ Hz)	11.42
H8	7.66–7.86 (m, 4H)	7.90	7.83–7.86 (m, 4H)	8.02
H9	7.23–7.41 (m, 4H)	7.69	7.46–7.49 (m, 4H)	7.79
H10	7.23–7.41 (m, 4H)	7.62	7.46–7.49 (m, 4H)	7.88
H11	7.66–7.86 (m, 4H)	8.09	7.83–7.86 (m, 4H)	8.28
H15	7.66–7.86 (m, 4H)	7.90	7.83–7.86 (m, 4H)	8.13
H16	7.23–7.41 (m, 4H)	7.69	7.46–7.49 (m, 4H)	8.02
H17	7.23–7.41 (m, 4H)	7.62	7.46–7.49 (m, 4H)	8.00
H18	7.66–7.86 (m, 4H)	8.09	7.83–7.86 (m, 4H)	8.51
H22	–	–	6.81 (s, 2H)	7.12
H24	–	–	6.81 (s, 2H)	7.36
H26 ^a	–	–	2.57 (s, 6H)	2.70
H27 ^a	–	–	2.19 (s, 3H)	2.36
H28 ^a	–	–	2.57 (s, 6H)	2.92

Note: the atom numbering according to Fig. 2 used in the assignment of chemical shifts.

^a Average.

at 8.37 and 8.03 ppm theoretically. A broad peak at 13.01 ppm may be assigned to the $-\text{NH}$ protons, which has been calculated at 9.01 ppm.

In the ^1H NMR spectra of compound **2**, the mesitylene backbone hydrogen's were appeared as three singlets at 2.19 ppm for $-\text{H}_{27}$, at 2.57 ppm for $-\text{H}_{26,28}$ and at 6.81 for $-\text{H}_{22,24}$ that have been observed at 2.36 ppm $-\text{H}_{27}$, at 2.70 ppm for $-\text{H}_{26}$, at 2.92 ppm for $-\text{H}_{28}$, at 7.12 ppm for $-\text{H}_{22}$ and at 7.36 ppm for $-\text{H}_{24}$ in the theoretical spectra. The $-\text{H}_{\text{benzimidazole}}$ peaks give two multiples around 7.46–7.49 ppm and 7.83–7.86 ppm while the pyridine backbone hydrogen's were observed as triplet at 8.39 ppm for $-\text{H}_{3A}$ and as doublets at 8.52 ppm for $-\text{H}_{2A,4A}$. The $-\text{NH}$ protons were identified at 10.28 ppm as broad peak, which have been computed in the region 9.64–19.34 ppm.

In the ^{13}C NMR spectra of compound **2**, there are two aliphatic peaks at 20.27 and 22.71 ppm for C_{27} and $\text{C}_{26,28}$, respectively. These signals have been calculated as 23.68 ppm for C_{27} , 27.10 ppm for C_{26} and 24.69 ppm for C_{28} . The peaks belonging to the rest of the

mesitylene backbone carbons were observed at 124.65, 136.05, 137.02 and 139.92 ppm, while the carbon peaks belonging to the benzimidazole backbone were observed at 115.29, 130.13 and 148.64 ppm. The pyridine backbone carbons were appeared in the region 123.30–145.34 ppm. These signals have been calculated in the range of 131.20–150.86 ppm, respectively. The individual experimental and theoretical chemical shift values can be seen in Table 5.

Electronic absorption spectra

The UV–vis. absorption spectra of the two compounds in methanol were recorded at room temperature within the 200–500 nm range and shown in Fig. 4. The two compounds have absorption in the range of 200–360 nm. In the spectra of compounds, four transitions (at 310, 301, 240 and 223 nm) for compound **1** and two transitions (at 311 and 206 nm) for compound **2** were observed, which can be assigned to $\pi \rightarrow \pi^*$ transitions. There is

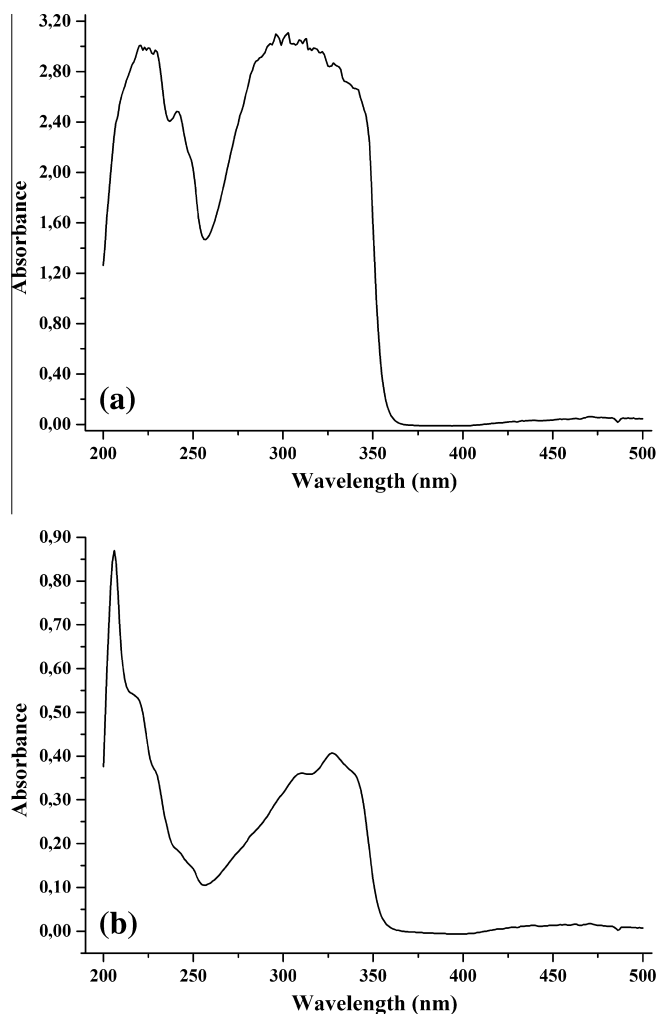


Fig. 4. UV-vis. spectra of compounds **1** (a) and **2** (b) in methanol.

one extra peak observed at 327 nm for compound **2**, which probably arises from charge transfer.

Electronic absorption spectra of the two compounds have been calculated by the TD-DFT method at the same level based on the optimized structure. The TD-DFT calculations in methanol solvent were performed by using the IEF-PCM solvation model. The calculated results are listed in Table 6 together with the experimental data. Three absorption bands at 319, 301 and 225 nm for compound **1** and two absorption bands at 335 and 316 nm for compound **2** were found. From Table 6, it can be seen that the theoretically calculated values suggest an acceptable agreement with the recorded spectral data.

Table 6
Experimental and electronic absorption spectra values for compounds **1** and **2**.

Compound	Experimental		Calculated	
	Wavelength (nm)	Abs.	Wavelength (nm)	Oscillator strength
1	223	2.993	225	0.104
	240	2.465	–	–
	301	3.082	301	0.566
	310	3.044	319	0.566
2	206	0.870	–	–
	311	0.361	316	0.399
	327	0.407	335	0.447

Conclusions

In this study, a novel benzimidazole salt compound (**2**) have been synthesized unexpectedly by the reaction of 2,6-bis(benzimidazol-2-yl)pyridine (**1**) with 2-mesitylenesulfonyl chloride in basic conditions while we plan to synthesize 2,6-bis{1-(mesitylsulfonyl)-1*H*-benzo[*d*]imidazol-2-yl}pyridine compound. Compounds **1** and **2** have been characterized by spectroscopic (FT-IR, NMR and UV-vis.) technique and single-crystal X-ray diffraction technique has been employed for the structural characterization of compound **2**. In addition, computational studies have been performed employing B3LYP hybrid density functional method with the 6-311G(d,p) basis set. When the experimental and theoretical results are compared, good correlations are found between them. The major discrepancies can mainly attributed to the solid state interactions in the crystal structure which are absent in the quantum mechanical modeling of the compounds.

Acknowledgements

This research has been supported by The Scientific and Technical Research Council of Turkey (TUBİTAK) (Project No: 107T808). We wish to thank Prof. Dr. Orhan Büyükgüngör for his help with the data collection and acknowledge the Faculty of Arts and Sciences, Ondokuz Mayıs University, Turkey, for the use of the STOE IPDS II diffractometer (purchased under Grant No. F-279 of the University Research Fund).

Appendix A. Supplementary material

CCDC 802607 contains supplementary crystallographic data (excluding structure factors) for the compound reported in this article. These data can be obtained free of charge at <http://www.ccdc.cam.ac.uk/cgi-bin/catreq.cgi> [or from the Cambridge Crystallographic Data Centre (CCDC), 12 Union Road, Cambridge CB2 1EZ, UK; fax: +44 (0)1223 336033; e-mail: deposit@ccdc.cam.ac.uk]. Supplementary data associated with this article can be found, in the online version, at <http://dx.doi.org/10.1016/j.saa.2014.04.148>.

References

- [1] A. Togni, L.M. Venanzi, *Angew. Chem. Int. Ed. Engl.* **33** (1994) 497–526.
- [2] S. Yamada, *Coord. Chem. Rev.* **190–192** (1999) 537–555.
- [3] F. Fache, E. Schulz, M.L. Tommasino, M. Lemaire, *Chem. Rev.* **100** (2000) 2159–2232.
- [4] M. Haga, in: J.A. McCleverty, T.J. Meyer (Eds.), *Comprehensive Coordination Chemistry II*, vol. 1, Pergamon Press, 2003, pp. 125–134.
- [5] B. Clercq, F. Verpoort, *Adv. Synth. Catal.* **344** (2002) 639–648.
- [6] S. Alper, Ö. Temiz-Arpaci, E. Şener, İ. Yaçın, *İ Farmaco* **58** (2003) 497–507.
- [7] C. Bailly, *Curr. Med. Chem.* **7** (2000) 39–58.
- [8] M. Del Poeta, D.L. Toffaletti, T.H. Rude, C.C. Dykstra, J. Heitman, J.R. Perfect, *Genetics* **152** (1999) 167–178.
- [9] D. Goodsell, R.E. Dickerson, *J. Med. Chem.* **29** (1986) 727–733.
- [10] R.V. Shingalapur, K.M. Hosamani, R.S. Keri, *Eur. J. Med. Chem.* **44** (2009) 4244–4248.
- [11] H.M. Refaat, *Eur. J. Med. Chem.* **45** (2010) 2949–2956.
- [12] H. Göker, C. Kuş, D.W. Boykin, S. Yıldız, N. Altanlar, *Biorg. Med. Chem.* **10** (2002) 2589–2596.
- [13] S. Özden, D. Atabey, S. Yıldız, H. Göker, *Biorg. Med. Chem.* **13** (2005) 1587–1597.
- [14] Z.M. Nofal, H.H. Fahmy, H.S. Mohamed, *Arch. Pharm. Res.* **25** (2002) 250–257.
- [15] O. Oter, K. Ertekin, O. Dayan, B. Çetinkaya, *J. Fluoresc.* **2** (2008) 269–276.
- [16] C. Sahin, Th. Dittrich, C. Varlikli, S. Icli, M.Ch. Lux-Steiner, *Sol. Energy Mater. Sol. C* **94** (2010) 686–690.
- [17] V.G. Vaidyanathan, B.U. Nair, *Eur. J. Inorg. Chem.* **18** (2005) 3756–3759.
- [18] S. Ruile, O. Kohle, P. Pechy, M. Graetzel, *Inorg. Chim. Acta* **261** (1997) 129–140.
- [19] K. Terada, K. Kobayashi, M. Haga, *Dalton Trans.* **36** (2008) 4846–4854.
- [20] O. Dayan, S. Dayan, İ. Kani, B. Çetinkaya, *Appl. Organomet. Chem.* **26** (2012) 663–670.
- [21] O. Dayan, N. Özdemir, Z. Şerbetçi, M. Dinçer, B. Çetinkaya, O. Büyükgüngör, *Inorg. Chim. Acta* **392** (2012) 246–253.

- [22] S. Günnaz, N. Özdemir, S. Dayan, O. Dayan, B. Çetinkaya, *Organometallics* 30 (2011) 4165–4173.
- [23] F. Zeng, Z. Yu, *Organometallics* 27 (2008) 2898–2901.
- [24] W. Addison, P.J. Burke, *J. Heterocycl. Chem.* 18 (1981) 803–805.
- [25] G.M. Sheldrick, SHELXS-97, Program for the Solution of Crystal Structures, University of Göttingen, Germany, 1997.
- [26] G.M. Sheldrick, SHELXL-97, Program for Crystal Structures Refinement, University of Göttingen, Germany, 1997.
- [27] L.J. Farrugia, *J. Appl. Crystallogr.* 30 (1999) 837–838.
- [28] Stoe, Cie, X-AREA Version 1.18 and X-RED32 Version 1.04, Stoe & Cie, Darmstadt, Germany, 2002.
- [29] A.L. Spek, *Acta Crystallogr. D65* (2009) 148–155.
- [30] L.J. Farrugia, *J. Appl. Chem.* 30 (1997) 565.
- [31] H.B. Schlegel, *J. Comput. Chem.* 3 (1982) 214–218.
- [32] C. Peng, P.Y. Ayala, H.B. Schlegel, M.J. Frisch, *J. Comput. Chem.* 17 (1996) 49–56.
- [33] R. Dennington II, T. Keith, J. Millam, Gauss View, Version 4.1.2, Semichem Inc., Shawnee Mission, KS, 2007.
- [34] M.J. Frisch, G.W. Trucks, H.B. Schlegel, G.E. Scuseria, M.A. Robb, J.R. Cheeseman, J.A. Montgomery Jr., T. Vreven, K.N. Kudin, J.C. Burant, J.M. Millam, S.S. Iyengar, J. Tomasi, V. Barone, B. Mennucci, M. Cossi, G. Scalmani, N. Rega, G.A. Petersson, H. Nakatsuji, M. Hada, M. Ehara, K. Toyota, R. Fukuda, J. Hasegawa, M. Ishida, T. Nakajima, Y. Honda, O. Kitao, H. Nakai, M. Klene, X. Li, J.E. Knox, H.P. Hratchian, J.B. Cross, V. Bakken, C. Adamo, J. Jaramillo, R. Gomperts, R.E. Stratmann, O. Yazyev, A.J. Austin, R. Cammi, C. Pomelli, J.W. Ochterski, P.Y. Ayala, K. Morokuma, G.A. Voth, P. Salvador, J.J. Dannenberg, V.G. Zakrzewski, S. Dapprich, A.D. Daniels, M.C. Strain, O. Farkas, D.K. Malick, A.D. Rabuck, K. Raghavachari, J.B. Foresman, J.V. Ortiz, Q. Cui, A.G. Baboul, S. Clifford, J. Cioslowski, B.B. Stefanov, G. Liu, A. Liashenko, P. Piskorz, I. Komaromi, R.L. Martin, D.J. Fox, T. Keith, M.A. Al-Laham, C.Y. Peng, A. Nanayakkara, M. Challacombe, P.M.W. Gill, B. Johnson, W. Chen, M.W. Wong, C. Gonzalez, J.A. Pople, Gaussian 03, Revision E.01, Gaussian Inc, Wallingford CT, 2004.
- [35] P. Hohenberg, W. Kohn, *Phys. Rev. B* 136 (1964) 864–871.
- [36] A.D. Becke, *J. Chem. Phys.* 98 (1993) 5648–5652.
- [37] C. Lee, W. Yang, R.G. Parr, *Phys. Rev. B* 37 (1988) 785–789.
- [38] A.D. McLean, G.S. Chandler, *J. Chem. Phys.* 72 (1980) 5639–5648.
- [39] K. Raghavachari, J.S. Binkley, R. Seeger, J.A. Pople, *J. Chem. Phys.* 72 (1980) 650–654.
- [40] M.P. Andersson, P. Uvdal, *J. Phys. Chem. A* 109 (2005) 2937–2941.
- [41] R. Ditchfield, *J. Chem. Phys.* 56 (1972) 5688–5691.
- [42] K. Wolinski, J.F. Hilton, P. Pulay, *J. Am. Chem. Soc.* 112 (1990) 8251–8260.
- [43] E. Cancès, B. Mennucci, J. Tomasi, *J. Chem. Phys.* 107 (1997) 3032–3041.
- [44] R.E. Stratmann, G.E. Scuseria, M.J. Frisch, *J. Chem. Phys.* 109 (1998) 8218–8224.
- [45] M.E. Casida, C. Jamorski, K.C. Casida, D.R. Salahub, *J. Chem. Phys.* 108 (1998) 4439–4449.
- [46] H. Xiao, G. Wang, F. Jian, *Acta Crystallogr. C66* (2010) o446–o448.
- [47] E. Freire, S. Baggio, J.C. Muñoz, R. Baggio, *Acta Crystallogr. C59* (2003) o259–o262.
- [48] M. Boča, D. Valigura, I. Svoboda, H. Fuess, W. Linert, *Acta Crystallogr. C56* (2000) 838–839.
- [49] B. Chetia, P.K. Iyer, *Tetrahedron Lett.* 47 (2006) 8115–8117.
- [50] S.M. Aucott, S.H. Dale, M.R.J. Elsegood, K.E. Holmes, L.M. Gilby, P.F. Kelly, *Acta Crystallogr. C61* (2005) o134–o137.
- [51] V.A. Russell, M.D. Ward, *J. Mater. Chem.* 7 (1997) 1123–1133.
- [52] J. Bernstein, R.E. Davis, L. Shimoni, N.-L. Chang, *Angew. Chem., Int. Ed. Engl.* 34 (1995) 1555–1573.
- [53] L.J. Bellamy, *The Infrared Spectra of Complex Molecules*, vol. 2, Chapman and Hall, London, 1980.
- [54] R.M. Silverstein, F.X. Webster, D.J. Kiemle, *Spectrometric Identification of Organic Compounds*, John Wiley and Sons, New York, 2005.